EEET ECOLOGICAL ENGINEERING & ENVIRONMENTAL TECHNOLOGY

Ecological Engineering & Environmental Technology, 2025, 26(9), 121–137
https://doi.org/10.12912/27197050/209558
ISSN 2719–7050, License CC-BY 4.0

Received: 2025.07.15
Accepted: 2025.08.16
Published: 2025.09.01

Land-use land-cover change analysis using remote sensing and geographic information systems in northen Rif, Morocco

Mustapha El Yousfi[1*], Abdelouafi El Ghoulbzouri[1], Mahjoub Himi[2]

[1] Laboratory of Applied Sciences, National School of Applied Science of Al Hoceima, Abdelmalek Essaadi University, Tetouan, Morocco
[2] Faculty of Earth Sciences, University of Barcelona, Spain
* Corresponding author's e-mail: ms.elyousfi@gmail.com

ABSTRACT

Land use and land cover (LULC) maps play a crucial role in guiding planning and management efforts, this study present consideration of regarding trend analysis in the land use and land cover of the Al Hoceima in the northern-central Rif region over a span of 25 years, from 2000 to 2025. For this purpose, a series of Landsat images, namely an Enhanced Thematic Mapper Plus (ETM+) image from 2000, Landsat 8 operational land imager (OLI) image from 2014, and a Landsat 9 Operational Land Imager (OLI) image from 2025 were obtained and processed using GIS and RS Software tools. Supervised classification with the maximum likelihood (ML) algorithm was applied to generate LULC maps. 120 ground truth points for each classified image were used to conduct accuracy evaluations, with overall accuracy ranging from 87.5% to 90.8% and Kappa coefficient ranging from 0.82 to 0.87. In order to examine and analyze the changes in LULC, we conducted a post-classification comparison. The findings revealed clear trends of decreasing in forests and dense vegetation areas at the expense of other classes. Additionally, there was a slight increase in the built-up area, which is likely driven by population growth and rising economic activity.

Keywords: land use/land cover, landsat, change detection, supervised classification, geographic information systems, remote sensing, maximum likelihood algorithm.

INTRODUCTION

The Earth's surface is continuously changing because of both natural and human-related processes, in this regard land use and land cover change plays a significant role (El Idrissi et al., 2024; Prestele et al., 2017). The resources of earth is becoming more scarcer due to the demographic, climatic and agricultural pressure (Bhargava, 2019; FAO, 2022; Pimentel, 1991; Tariq, 2024). Planning for the environment, making data-driven decisions, and managing land sustainably all depend on an understanding of changes in land use and land cover (LULC) (He et al., 2019; Nunez and Alkemade, 2021; Oliver and Morecroft, 2014).

Numerous studies have investigated land use and land cover (LULC) changes across various regions of Morocco using geographic information systems (GIS) and remote sensing (RS) techniques, highlighting trends such as forest loss and urban expansion (Ben-Said et al., 2025). Ben-Said et al. 2025 provide a comprehensive review of the national literature and highlight important gaps, such as the absence of multi-decadal studies in some areas, insufficient consideration of climate change, and limited analyses linking LULC changes to natural hazards.

The study area represents a complex landscape which is characterized by its diverse geologic formations, its rich biodiversity and its ecological and cultural importance. This area remains understudied in terms of LULC dynamics, especially over multi-decadal timescales. Moreover, the region has recently experienced increased climatic stress, including long

drought periods over the last 20 years, which could have sped up changes in patterns of land cover and land use.

Additionally, the study area is highly prone to landslides -due to its complex geology, steep slopes, and intense rainfall events-, which are frequently made worse by changes in land use. Therefore, it is crucial for disaster risk reduction and sustainable land management in this vulnerable area to comprehend how LULC dynamics influence landslide susceptibility.

The present study intends to fill in these knowledge gaps and deepen our understanding of LULC changes in the central Rif. By applying advanced RS and GIS techniques combined with statistical analyses, we seek to detect and quantify LULC trends over a 25-year period, and to identify the primary drivers of these changes. Particularly, we expect that human interventions and climate variability have significantly altered and changed land use patterns, leading to measurable shifts in ecosystem composition and land management practices.

Through this research, we aim to provide new scientific insights and knowledge into the spatial-temporal dynamics of LULC in an under-investigated region of Morocco, contributing to improved land planning, disaster risk management, and sustainable resource policies tailored to the central Rif context.

METHODS AND METHODOLOGY

Study Area

This study focuses on an area situated in the north of Morocco, it includes the province of Al Hoceima and the western parts of the province of Driouch (Figure 1). It covers an area of 4383,914 km² (438391,4 ha) in the northern Rif. The study area lies between longitude 04°50’ W to 03°30’ W and latitude 34°40’ N to 35°20’ N, it is bordered on the north by the Mediterranean Sea, on the west by Chefchaouen province, and on the south by Taounate province.

The area is recognized for its Mediterranean climate, which features two seasons, dry and humid, (Driouech et al., 2021). The average annual rainfall in the area varies between 300 mm to over 400 mm. (Muselli et al., 2022; Salhi et al., 2019), the eastern parts of the region, especially the basins between Jebha and Al Hoceima, receives slightly more rainfall than the western areas. The region is characterized by mountainous landforms with steep

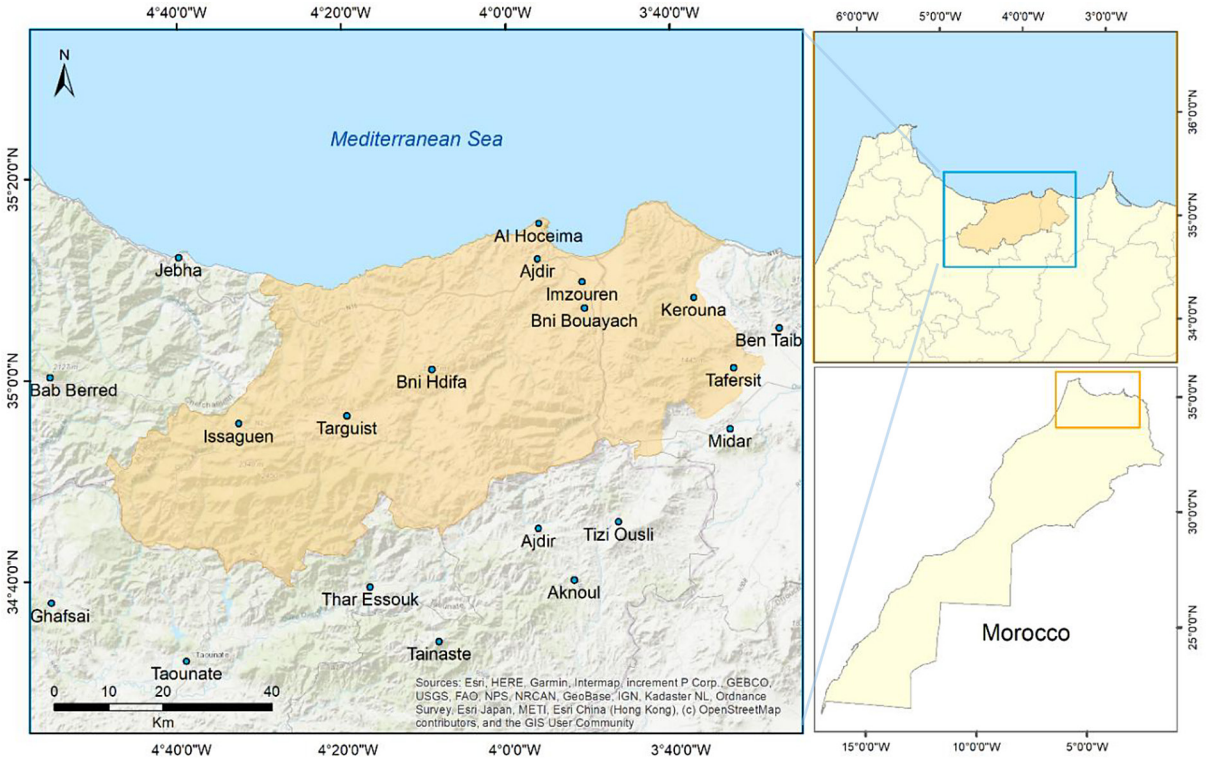

Figure 1. Study area map

slopes, which leads in addition to torrential rain, to erosion and changes in vegetation and land cover (Mouddou et al., 2024).

From a geological and geomorphological perspective, the study area makes part of the internal Rif and flyshs domains (Suter, 1980; Michard et al., 2008). The Study area is well-known by its geological and natural environments. Cedar trees predominate in the forests and rich ecosystems found at high altitudes in the southwest parts (Abel-Schaad et al., 2018).

Data collection and pre-processing

Three Landsat images at a resolution of 30m, including one enhanced thematic mapper plus (ETM+) image from 25 April 2000, one Landsat 8 operational land imager (OLI) image from 27 June 2014, and one Landsat 9 OLI image from 16 May 2025 (Table 1), were obtained from the United States Geological Survey (USGS) website (http://earthexplorer. usgs.gov/). All the three images have 0% cloud coverage, we chose to acquire the images from April to June due to the reduced cloud cover and the availability of fresh green vegetation, which makes it easier to distinguish different land cover types and analyze changes in vegetation.

The datasets were acquired as TIF files with separated bands, to start working on the images a layer stack tool is used to combine the bands altogether; (bands 1, 2, 3, 4, 5, 7 for Landsat 7 image and Bands 2, 3, 4, 5, 6, 7 for Landsat 8 and 9 images). and create one stacked image (Bruce and Hilbert, 2004), the Figure 2 shows the three satellite images subsided into study area in different band combinations.

Preprocessing is necessary for satellite image analysis, it serves to improve spectral separability and facilitate visual interpretation of Earth's surface features and to enhance the quality of inputs used in automated image processing (Pacheco et al., 2023; Rasmussen, 1993).

The preprocessing tasks were conducted using the open source quantum GIS (QGIS) software (Version 3.24) (QGIS Development Team, 2024) and ArcMap software (Version 10.8.2) (Esri, 2020).

Geometric correction and radiometric correction are the two forms of correction required for appropriate satellite image analysis (Rasmussen, 1993), and because all the satellite images used in this study are at Level 1, which means that the information had already been orthorectified (Roy et al., 2014) there will be no need for geometric correction (Storey et al., 2014).

To enhance visibility and analysis, radiometric correction was applied to boost satellite image's brightness and magnitude, (through the plugin "Radiometric calibration") (Chavez Jr, 1989; Teillet et al., 1982).

Radiometric calibration is used to translate digital numbers (DNs) into top atmosphere (TOA) radiance values (Chavez Jr, 1989; Roy et al., 2014; Teillet et al., 1982). And then the atmospheric correction was done with the help of the Semi-Automatic Classification Plugin (Congedo, 2016), based on the dark object subtraction (DOS) approach (Chavez, 1988) in order to obtain TOA reflectance, using the equation (Chavez, 1996):

$$L_{\mathrm{p},\lambda} = L_{s,\lambda} - L_{\mathrm{min}} \quad (1)$$

where: $L_{p\lambda}$ – corrected radiance at wavelength λ after removing atmospheric effects, $L_{s\lambda}$ – sensor-received radiance at wavelength λ, L_{min} – minimum (or dark object) radiance.

Once the TOA reflectance values have been calculated, we performed Pansharpening using NNDiffuse method (QGIS verify) that involves combining high-resolution panchromatic imagery (band 8, 15 m) with multispectral imagery (30 m) to create a single higher-resolution, and visually appealing composite image.

Pansharpening techniques combine the high-resolution spatial details from the panchromatic band with the rich color information from the multispectral bands to enhance the spatial resolution of the resulting composite image. This

Table 1. Satellite images used in the study

Image type	Date	Spatial resolution	Cloud cover
ETM+	2000/04/25	30 m	0%
OLI	2014/06/27	30 m	0%
OLI	2025/05/16	30 m	0%

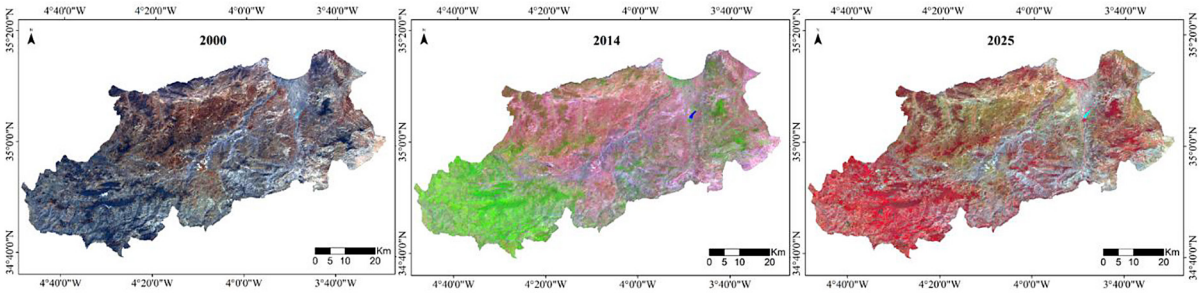

Figure 2. The three satellite images subsided into study area in different band combinations. 2000: Natural color, 2014: False color, 2025: Color infrared

high-resolution composite image of 15 m is then subset into the study area using "extract by mask tool" in ArcMap in order to enhance the speed of the image processing and analysis.

For this study, we performed radiometric calibration by converting DN to TOA reflectance, then we applied DOS reflectance to obtain surface reflectance from top atmosphere reflectance (TOA) in addition of contrast enhancement, we increased the resolution of the three satellite images from 30 m to 15 m using the panchromatic band which comes with a resolution of 15 m. To do this we applied pansharpening method using NNDiffuse method. Google Earth images, along with field data, were used to validate the proposed methodology. Fieldwork involved using GPS-based ground control points and previous knowledge to conduct ground truth surveys. The methodology followed in this study is illustrated in the flowchart presented in Figure 3.

Methodology

The principal aim of this study is to generate land use and land cover maps of the years 2000, 2014 and 2025 over a period of 25 years using satellite images, and to examine the identification of changes in the LULC. For precise mapping of LULC changes, the study uses the maximum likelihood (ML) algorithm, a technique that is commonly used in supervised classification (Abbas TAATI, 2015; Erbek et al., 2004; Jensen, 2016).

In land use land cover analysis, supervised classification requires labeled training samples to build a model for the purpose of classifying remote sensing data into predetermined land cover classes. (Talukdar et al., 2020; Vali et al., 2020). Using the spectrum properties of the training samples as a basis, the maximum likelihood algorithm quantifies the likelihood of each pixel being associated with a particular class, allocating the pixel to the class with the highest likelihood (Xie and Huang, 2022).

We adopted a five-class scheme to characterize physical land surface properties, including vegetation, built up areas, bare land, in order to assess and identify changes in land use and land cover (LULC) that have occurred during the last quarter decade (Table 2). This study's approach includes a number of crucial steps: (1) data pre-processing, (2) classification, (3) accuracy assessment, and (4) change detection, with several sub-steps.

Satellite images were processed, categorized, and analyzed using a variety of GIS and RS software applications, such as QGIS and ArcMap. ArcMap (version 10.8) was used to create thematic maps and perform extra area computations. Microsoft Excel was used to create tables,

Table 2. Classes of land use land cover adopted in the study

LULC categories	Description
Water	Water bodies, dams
Forest & dense vegetation	Dense forest including natural forests and planted trees
Shrubland & sparse vegetation	Low percentage of vegetation
Bare land	Open land, bare soil, bare rock areas
Urban & built-up area	Settlements, residential and urban areas

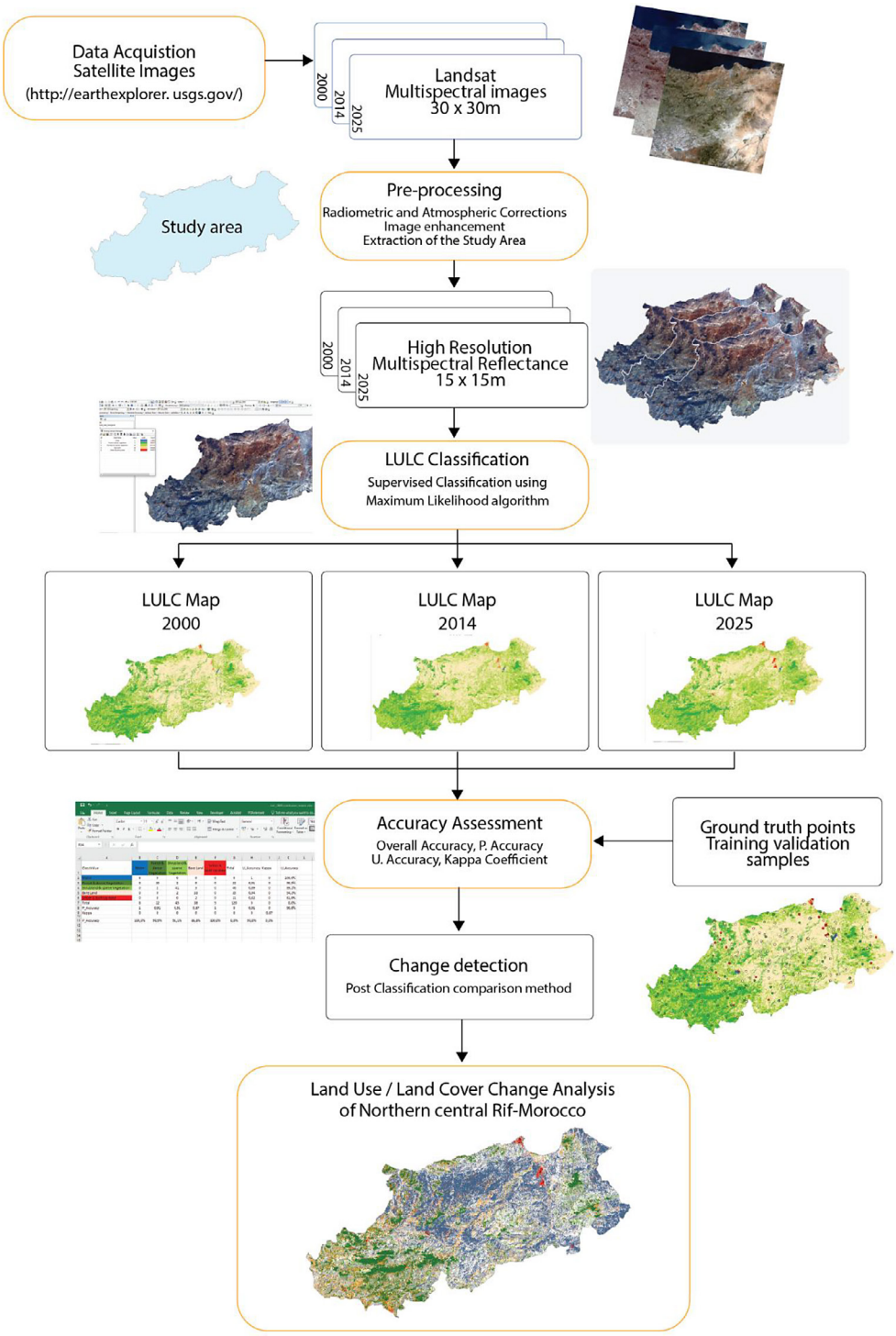

Figure 3. Flowchart – LULC mapping and change analysis process

calculate, and create graphs. The flow diagram for this study shows the processes (Figure 3).

Utilizing QGIS software version 3.24, pre-processing was done on the data for layer stacking, radiometric and atmospheric corrections. To improve the images quality, enhancement techniques are typically utilized. The subsetting process was performed using the "extract by mask" tool in ArcGIS 10.8 software. Then Landsat images of the years 2000, 2014 and 2025 were classified using a supervised classification approach based on the maximum likelihood algorithm. The LULC maps that were generated underwent statistical analysis using ArcGIS 10.8 software to determine and quantify changes in land use and land cover.

Image classification

In land use and land cover study, supervised classification is a commonly used technique, and the maximum likelihood algorithm is the most used in LULC classification and change analysis (Norovsuren et al., 2019). With this technique, the user defines the land cover classes and pre-classified sample data are used to train a classification algorithm. Based on the spectral properties extracted from the training data, the maximum likelihood method determines the statistical probability that each pixel belongs to a specific land cover class. The algorithm finds the most likely class for every pixel in the whole image by maximizing the chance that a pixel will be assigned to a particular class (Jensen, 2016).

To perform LULC Classification we adopted a five class scheme for the study area (Table 2), water bodies, forest and dense vegetation, shrubland and sparse vegetation, bare land and urban areas. The three Landsat images from 2000, 2014 and 2025 were classified using a supervised approach based on the maximum likelihood algorithm in order to perform a LULC classification. The classifying process is composed of three basic steps: 1. Training samples selection, 2. Classification, 3. Accuracy Assessment.

Representative samples of identified cover types are used to create a numerical signature, about 300 training samples were created for each map, the number of samples differs from a class to another depending on the geographical area occupied by each class, and then we applied the maximum likelihood technique using ML algorithm. The resulting LULC maps were analyzed using ArcMap software to determine the LULC changes in the study area.

Accuracy assessment

After image classification, accuracy evaluation is essential since it assesses the quality and confidence of the classification outcomes (Congalton, 1991; Maxwell et al., 2021; Anderson et al., 1976). Achieving a high degree of precision gives us the confidence to interpret land cover data, use the information for mapping hazards, urban planning, and natural resource management (Venter and Sydenham, 2021).

120 assessment points were randomly generated to calculate the accuracy for each map. to ensure the representation of all classes, a stratified random sampling was used to denote different LULC classes (Figure 4), then the appropriate class from ground truth is designated to each point using high-resolution Google Earth images and field data (Dong et al., 2020).

Confusion matrix for the classified images was obtained for the three satellite images (2000, 2014 and 2025); the confusion matrix evaluates the classification accuracy (Congalton and Green, 2008). This matrix gives a clear idea of a classification performance across several classes; it is a valuable tool for evaluating a model's efficacy.

When evaluating the effectiveness of classification models, a number of critical metrics are essential, such as overall accuracy, producer's accuracy, user's accuracy, and Kappa coefficient (Congalton and Green, 2008).

Producer's accuracy (PA), sometimes referred to as omission error, quantifies the likelihood that a ground pixel belonging to a specific land cover class is accurately categorized as such class on the map. It is calculated using the formula:

$$Producer's\ Accuracy = \\ = \frac{Number\ of\ True\ Positives}{Total\ Number\ of\ Actual\ Pixels\ for\ a\ Class} \times 100 \quad (2)$$

User's accuracy (UA), also referred to as commission error, assesses the probability that a pixel on the map assigned to a particular land cover class actually belongs to that class on the ground, the formula for User's Accuracy is:

$$User's\ Accuracy = \\ = \frac{Number\ of\ True\ Positives}{Total\ Number\ of\ Classified\ Pixels\ for\ a\ Class} \times 100 \quad (3)$$

Overall Accuracy refers to the percentage of pixels correctly classified across all land cover classes, and is given by the formula (Das and Sarkar, 2019):

$$Overall\ Accuracy = \\ = \frac{Number\ of\ Correctly\ Classified\ Pixels}{Total\ Number\ of\ Pixels} \times 100\ (\%) \quad (4)$$

Kappa coefficient (Cohen's Kappa) is a statistic that evaluates the degree of agreement between the classifications generated by a model and the classifications based on ground truth data, taking into consideration the possibility of chance agreement. Kappa coefficient is calculated by the formula:

$$Kappa\ Coefficient = \frac{P_o - P_e}{1 - P_e} \quad (5)$$

where: P_o represents the observed agreement, i.e., the proportion of agreement between the

model and reference classifications, P_e represents the expected agreement, i.e., the proportion of agreement expected by chance.

All these metrics and measures together offer a comprehensive evaluation of the accuracy and reliability of LULC classification models.

Change detection and analysis

Change detection in LULC involves identifying and analyzing shifts in the distribution and characteristics of various land cover categories over a certain time. This approach is essential for observing environmental transformations, assessing the impact of human activities, and analyzing how landscapes evolve over time (Cheng et al., 2023). Change detection can highlight changes and trends in land use, such as deforestation, urbanization,… etc., and can offer essential information for effective resource planning, hazards mapping and the promotion of sustainable land use management (Das and Angadi, 2022).

In this study the Post-classification comparison is used to analyze changes in LULC over 25 years, it involves comparing the classified land cover maps derived from remote sensing imagery for the years 2000, 2014 and 2025, the differences in class distribution were analyzed to identify areas of change.

First, we proceeded to analyze change detection between the years 2000 to 2014, then from 2014 to 2025 and from 2000 to 2025.

The classified LULC raster images were converted to vector layers as part of the post-classification process by using the conversion tools in ArcGIS. Then "intersect" of "geoprocessing" tools in ArcGIS was used to calculate change for each class and identify areas where land cover has changed between two periods by performing a pixel by pixel comparison.

This involves comparing the two maps, examining each pixel to figure out if the land cover class has changed or not.

RESULTS AND DISCUSSION

LULC patterns and distribution

The LULC pattern is characterized into five classes, water, forest/dense vegetation, shrubland/sparse vegetation, urban/built-up area and bare land. The results of classification and area distribution are shown in Table 3 and the Figure 5. These maps show the different LULC classes for 3 study years, (2000, 2014, and 2025) in the study area.

In 2000, the "bare land" class occupied the highest area with 1922.42 km² (43.85%) of the total area, while the "water" class was the least representative of the classes with only 2.24 km² (0.05%). This is due to the fact that the study area has only two small dams or reservoirs.

Forest and dense Vegetation covered an area of 22.9%, 17.64% and 17.54% during the years

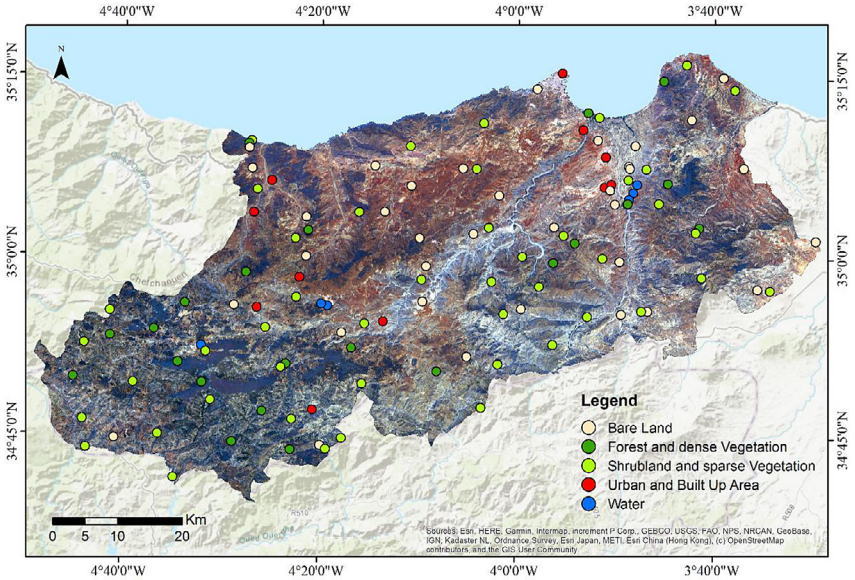

Figure 4. Map of randomly selected points for accuracy assessment of LULC map of the year 2025, shown on a true color Landsat image of 2025

2000, 2014 and 2025 respectively; on the other hand, urban and built-up area occupied 13.99 km² (0.32%) in 2000, 17.52 km² (0.4%) in 2014 and 32.33 km² (0.74%) in 2025.

The class "shrubland and sparse vegetation" was about 1441.4 km² (32.88%) in 2000, 1792.56 km² (40.89%) in 2014 and reaches 2132.22 km² (48.64%) in 2025; "bare land" occupied 1922.42 km² (43.85%) of the total area in 2000, then 1798.26 km² (41.02%) in 2014, and continues to shrink at the expense of other classes reaching 1448.33 km² (33.04%) in 2025.

"Water bodies" class stays almost unchangeable, the class covered 2.24 km² (0.05%) in 2000, 2.43 km² (0.06%) in 2014 and 2.17 km² (0.05%) in 2025.

Vegetation areas especially forests and dense vegetation play an important role in the environmental balance, hydrological process, and slope stability. However, based on the results we notice the decreasing in the area covered by forests and dense vegetation from 22.9% (in 2000) to 17.54% (in 2025).

On the other hand, there were a slight increase in built-up area, from 0.32% of the total area in 2000 to 0.74% in 2025, which is a normal trend in response to the increase in the population.

Accuracy assessment of classified images

The classification results for each LULC class were evaluated using error matrices. Total of 120 ground truth points were identified for every LULC map. In this research user's accuracy, overall accuracy, producer's accuracy, and kappa (κ) statistics were evaluated through error matrix analysis.

Details of these metrics values of the classified images of the years 2000, 2014 and 2025 are shown in Tables 4, 5 and 6.

In 2000, producer accuracy was 100% for water, 91.3% for forest/dense vegetation, 84.8% for shrubland / sparse vegetation, 84.3% for bare land and 100% for urban / built-up area. while user's accuracy for the same year was 100% for water, 84% for forest / dense vegetation, 80% for shrubland / sparse vegetation, 95.6% for bare land and 80% for urban / built-up area (Table 4).

In 2014, producer accuracy was 100% for water, 95.5% for forest / dense vegetation, 85% for shrubland / sparse vegetation, 86.4% for bare land and 100% for urban / built-up area. while User's accuracy for the same year was 100% for water, 91.3% for forest / dense vegetation, 87.2% for shrubland / sparse vegetation, 90.5% for bare land and 83.3% for urban / built-up area (Table 5).

In 2025, producer accuracy was 100% for water, 90.9% for forest / dense vegetation, 91.1% for shrubland / sparse vegetation, 86.8% for bare land and 100% for urban / built-up area. While user's accuracy for the same year was 100% for water, 90.9% for forest / dense vegetation, 89.1% for shrubland / sparse vegetation, 94.3% for bare land and 81.8% for urban / built-up area (Table 6).

The overall classification accuracy for the years studied was 87.5% for 2000, 89.2% for 2014 and 90.8% for 2025 in the study area. Kappa coefficient (κ) for 2000, 2014, and 2025 were 0.82, 0.85 and 0.87 respectively.

LULC change detection

After classification, we obtained three LULC maps for three years 2000, 2014 and 2025. These maps with the use of Post-classification comparison leads us to detect the changes that took place over the past twenty-five years. Changes in land use and land cover between 2000 to 2014, 2014 to 2025, and 2000 to 2025 was attained (Figures 6, 7, 8, 9 and 10).

We notice a noticeable decrease in the dense vegetation areas and forests for the benefit of other classes. Moreover, a slight increase in the built

Table 3. Area distribution of the years (2000, 2014 and 2025)

LULC classes	2000		2014		2025	
	Sq. km	%	Sq. km	%	Sq. km	%
Water	2.24	0.05	2.43	0.06	2.17	0.05
Forest & dense veg.	1003.83	22.9	773.11	17.64	768.84	17.54
Shrubland & sparse vegetation	1441.41	32.88	1792.56	40.89	2132.22	48.64
Bare land	1922.42	43.85	1798.26	41.02	1448.33	33.04
Urban & built up area	13.99	0.32	17.52	0.4	32.33	0.74
Total	4383.9	100	4383.9	100	4383.9	100

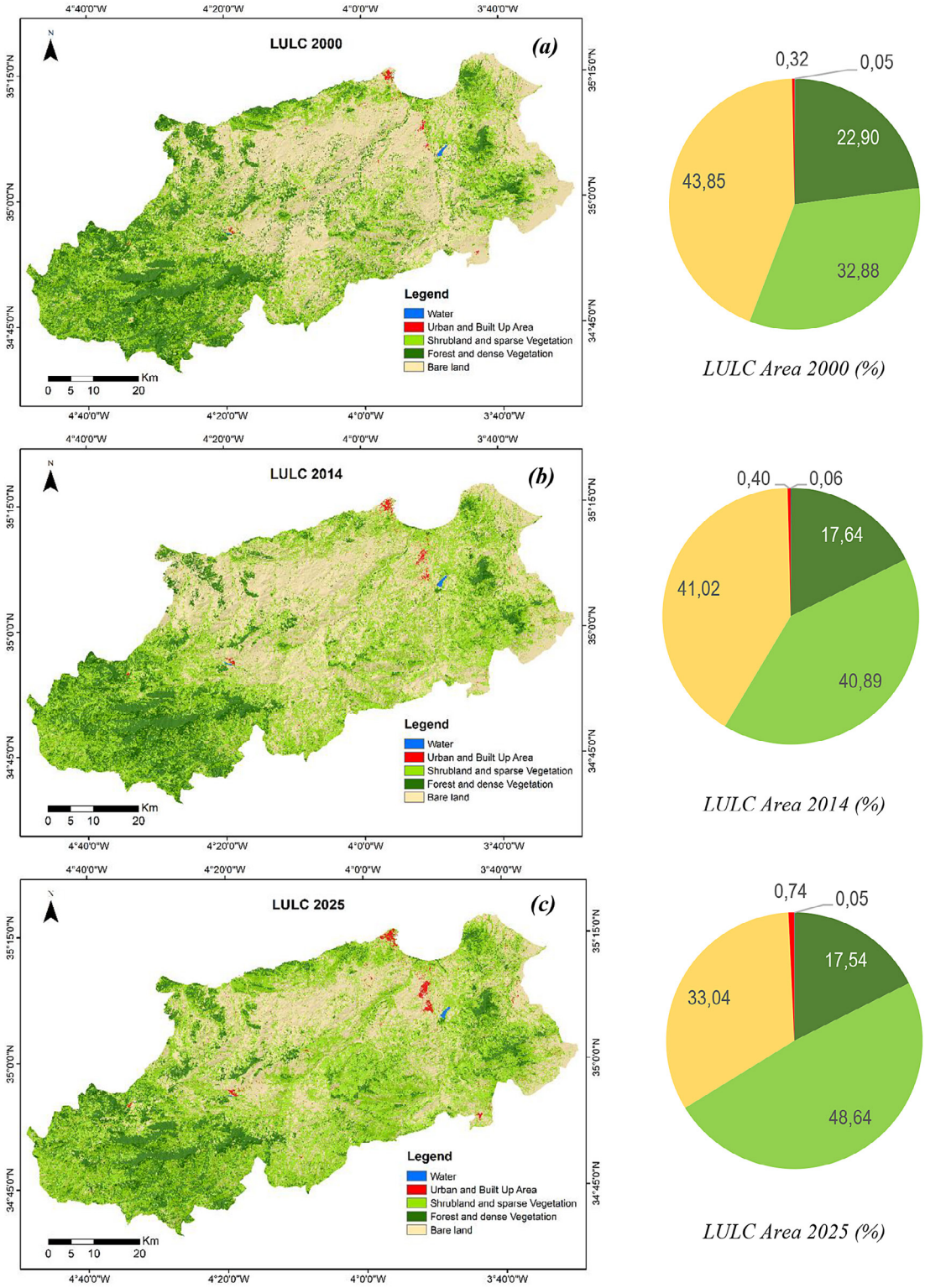

Figure 5. LULC maps and area distribution (a: 2000, b: 2014, c: 2025)

up area, which is due to the increase in population and economic activities.

2000 to 2014

In 2000, the "bare land" occupied the highest class with 1922.42 km² (43.85%), which decreased to 41.02% in 2014 (Table 7). Forest and dense vegetation class is showing a decrease form 1003.83 km² (22.9%) in 2000 to 773.1 km² in 2014 (17.64%), while shrubland and sparse vegetation knows an increase from 1441.41 km² (32.88%) in 2000 to 1792.56 km²

Table 4. Evaluation of accuracy (year 2000)

Classes	Water	Forest & dense vegetation	Shrubland & sparse vegetation	Bare land	Urban & built up area	Total	U Accuracy	Kappa
Water	5	0	0	0	0	5	1	
Forest & dense veg.	0	21	3	1	0	25	0.84	
Shrubland & sparse veg.	0	2	28	5	0	35	0.8	
Bare land	0	0	2	43	0	45	0.96	
Urban & built up area	0	0	0	2	8	10	0.8	
Total	5	23	33	51	8	120	0	
P accuracy	1	0.91	0.85	0.84	1	0	0.88	
Kappa								0.82

Table 5. Evaluation of accuracy (year 2014)

Classes	Water	Forest & dense vegetation	Shrubland & sparse vegetation	Bare land	Urban & built up area	Total	U accuracy	Kappa
Water	4	0	0	0	0	4	1	
Forest & dense veg.	0	21	2	0	0	23	0.91	
Shrubland & sparse veg.	0	1	34	4	0	39	0.87	
Bare land	0	0	4	38	0	42	0.90	
Urban & built up area	0	0	0	2	10	12	0.83	
Total	4	22	40	44	10	120	0	
P accuracy	1	0.95	0.85	0.86	1	0	0.89	
Kappa								0.85

Table 6. Evaluation of accuracy (year 2025)

Classes	Water	Forest & dense vegetation	Shrubland & sparse vegetation	Bare land	Urban & built up area	Total	U accuracy	Kappa
Water	6	0	0	0	0	6	1	
Forest & dense veg.	0	20	2	0	0	22	0.91	
Shrubland & sparse veg.	0	2	41	3	0	46	0.89	
Bare land	0	0	2	33	0	35	0.94	
Urban & built up area	0	0	0	2	9	11	0.82	
Total	6	22	45	38	9	120	0	
P accuracy	1	0.91	0.91	0.87	1	0	0.91	
Kappa								0.87

(40.89%) in 2014. Built-up area is showing a positive trend from 13.99 km² (0.32%) in 2000 to 17.52 km² (0.4%) in 2014, It has slightly increased by 3.53 km².

On the other hand, water bodies area remains almost unchanged (from 2.23 km² in 2000 to 2.43 km² in 2014). The built-up and urban areas was increased especially in the cities of Al Hoceima, Imzouren, Beni Bouayach and Targuist (Figure 6), due to the normal increase in population and due to migration from the countryside and rural areas.

2014 to 2025

Shrubland and sparse vegetation continue increasing from 1792.56 km² (40.89%) in 2014 to 2132.22 km² (48.64%) in 2025. Built-up area also continue showing a positive trend

from 17.52 km² (0.4%) in 2014 to 32.33 km² (0.74%) in 2025. Bare land shows a decrease from 1798.26 km² (41.02%) in 2014 to 1448 km² (33.04%) in 2025, this decrease is in general in favor of shrubland and sparse vegetation (Figure 7).

Forest and dense vegetation occupied 773.11 km² (17.64%) in 2014, which slightly decreased to 768.84 km² (17.54%) in 2025. While water class shows a very slight decrease from 2.43 km² (0.06%) in 2014 to 2.17 km² (0.05%) in 2025 (Table 8).

2000 to 2025

From 2000 to 2025, the evolution shows a negative trend in "forest and dense vegetation" area, this class lost 5.36% of its area during the last 25 years (Figure 8).

Bare land class also shows a decreasing from 2000 to 2025 by losing 10.8% of its area. While "shrubland and sparse vegetation" shows a positive trend, from 1441.41 km² (32.88%) in 2000 to 2132.22 km² (48.64%) in 2025, with an increase of 15.76%, this increase comes from bare land class and less from "forest and dense vegetation".

Built up area keeps showing a positive change from 2000 to 2025 (an increase of 18.34%) in the study area. The majority of this increase is concentrated in the urban areas due to internal migration from the countryside to the cities or villages (Figure 9).

Area covered by "water" which is the smallest class, remains almost unchangeable (0.05%). The Figure 10 shows the change trends and evolution of all the five classes analyzed in this study from 2000 to 2025 (Table 9).

DISCUSSION

Over the course of 25 years, our analysis showed that patterns of LULC had significantly changed from 2000 to 2025. The results show a dynamic evolution of the landscape marked by changes in the types of land cover, suggesting the influence of different natural and human forces.

The alterations observed in LULC are a result of both human activities and natural processes. Several trends were observed, among them forest degradation and urban expansion with observable increases in the built-up area at the expense of other land cover classes which aligns with trends observed and documented in previous studies (Gashu and Gebre-Egziabher, 2018; Naikoo et al., 2020; Patra et al., 2018).

Various factors contribute to the observed changes in LULC. Population expansion, drought periods, economic development, and infrastructure projects have accelerated the process of urbanization, resulting in the conversion of rural and natural landscapes into urban areas. Additionally, land cover changes have been impacted by factors such as climate, land management practices and strategies, and policy measures, which have contributed to the observed changes in LULC (Sang et al., 2023; Tan et al., 2024).

The sustainability of the environment and ecosystem services is significantly affected by land cover change. The loss of natural habitats and ecosystems can negatively affect soil fertility, water quality, and biodiversity, which in turn impacts ecosystem function and resilience (Millennium Ecosystem Assessment, 2005). Moreover, expanding urban areas increase the

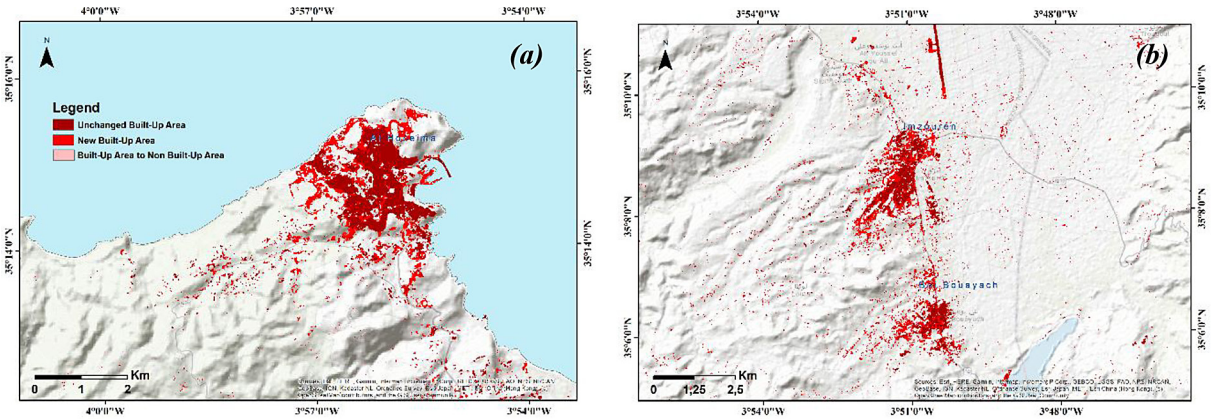

Figure 6. Change in built up area between 2000 and 2014 (a: city of Al Hoceima, b: Cities of Imzouren and Beni Bouayach)

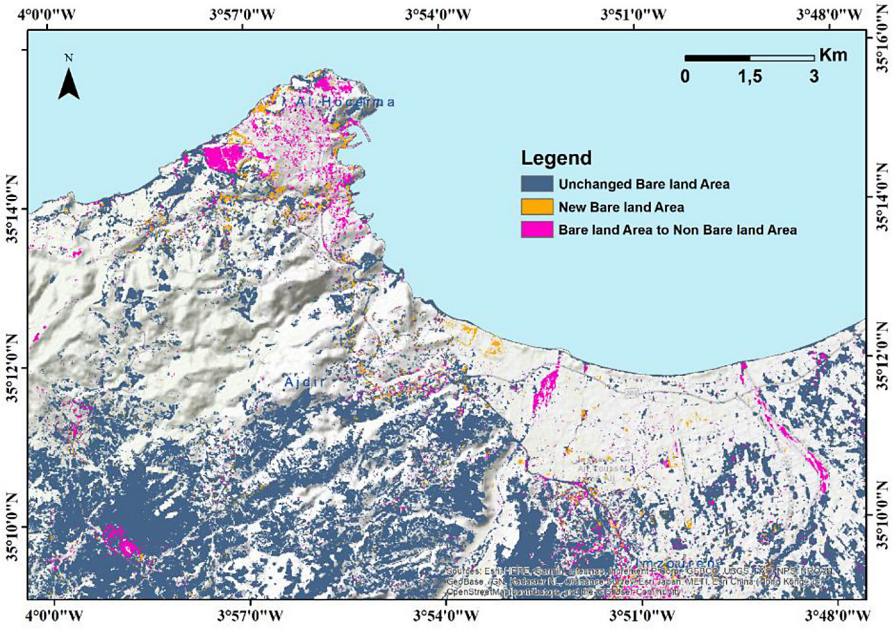

Figure 7. Change in bare land between 2014 and 2025 (City of Al Hoceima, Ajdir and parts of Nekor plain)

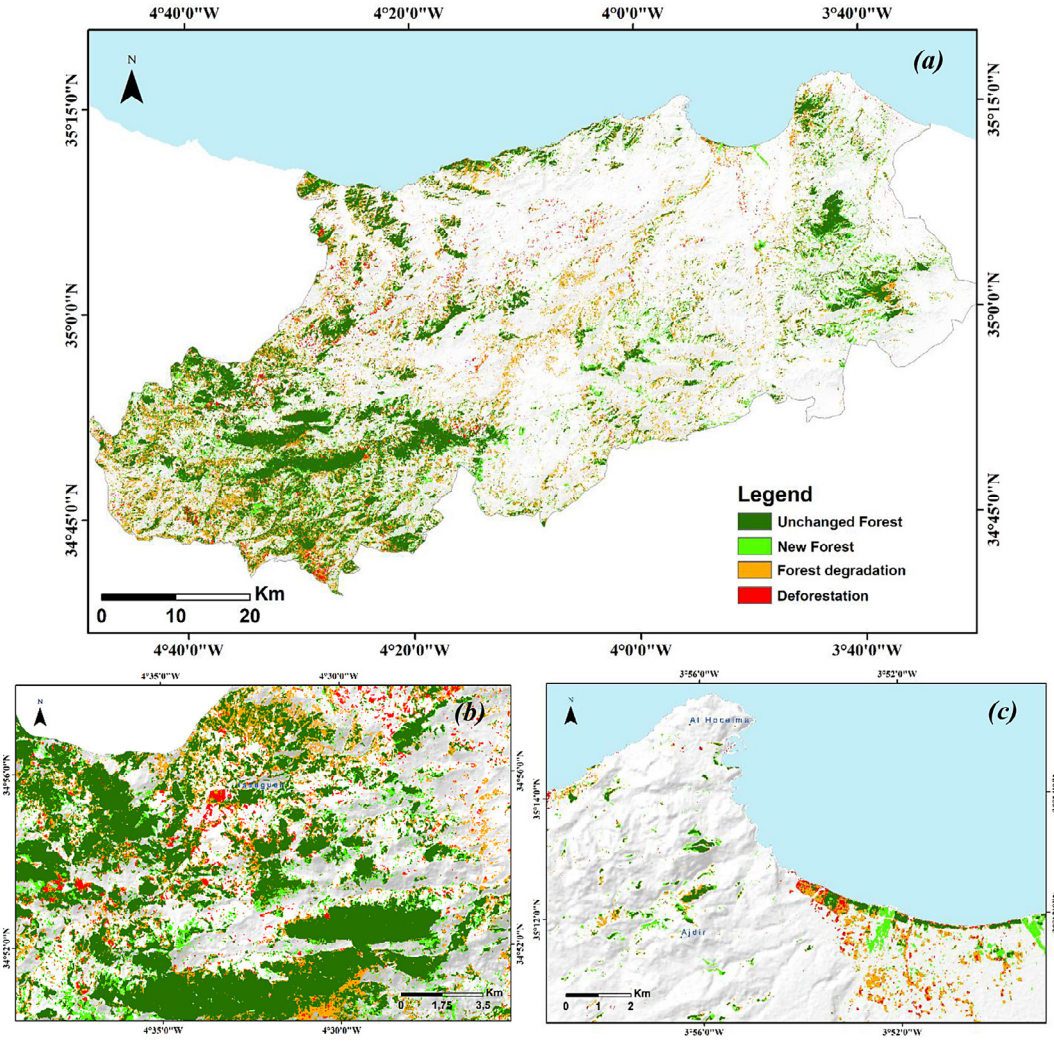

Figure 8. Change in forest and dense vegetation – Deforestation and forest degradation between 2000 and 2025 (a: Study area, b: Issaguen, c: Bay of Al Hoceima)

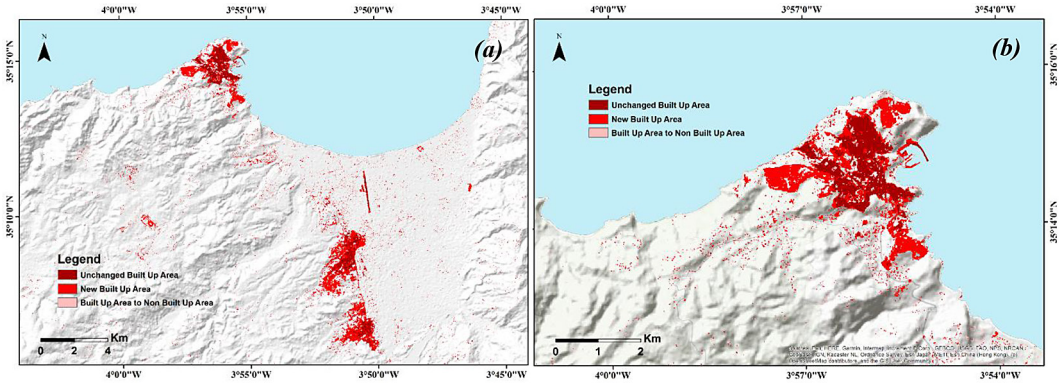

Figure 9. Change in built up area between 2000 and 2025 (a: Nekor Plain, b: City of Al Hoceima)

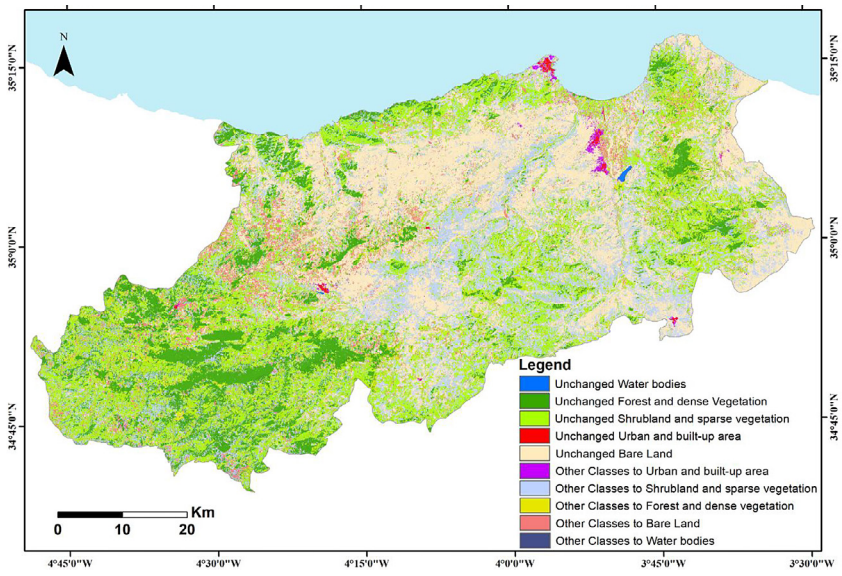

Figure 10. Change detection map from 2000 to 2025 in the study area

Table 7. Change assessment (2000 to 2014)

2014 (area in km²)							
2000 (area in km²)	Classes	Water	Forest & dense vegetation	Shrubland & sparse vegetation	Bare land	Urban & built up area	Total
	Water	2.11	0	0	0.1	0.02	2.23
	Forest & dense veg.	0.03	596.58	304.24	102.61	0.21	1003.7
	Shrubland & sparse veg.	0.01	163.21	962.77	313.68	1.61	1441.3
	Bare land	0.28	13.18	522.93	1375.65	10.21	1922.3
	Urban & built up area	0	0.07	2.45	6	5.47	13.99
	Total	2.43	773.04	1792.4	1798.04	17.52	4383.9

vulnerability of populations to environmental threats including pollution and flooding.

Furthermore, landslides investigations require good understanding of LULC dynamics and patterns. Changes in land cover can have a serious impact on soil stability which lead to increase the risk of landslides (Chen et al., 2019), This effect is most pronounced in case of forest degradation and urbanization. In order to protecting infrastructures and human lives, mapping changes in LULC helps identify areas which are vulnerable to landslides and supports

Table 8. Change assessment (2014 to 2025)

2025 (area in km²)							
2014 (area in km²)	Classes	Water	Forest & dense vegetation	Shrubland & sparse vegetation	Bare land	Urban & built up area	Total
	Water	2.04	0.02	0.17	0.19	0	2.43
	Forest & dense veg.	0	567.96	185.06	19.73	0.28	773.04
	Shrubland & sparse veg.	0.03	185.59	1302.98	297.93	5.88	1792.4
	Bare land	0.09	15.18	642.58	1123.02	17.2	1798.04
	Urban & built up area	0.01	0.01	1.23	7.32	8.95	17.52
	Total	2.17	768.76	2132	1448.17	32.33	4383.9

Table 9. Change assessment (2000 to 2025)

2025 (area in km²)							
2000 (area in km²)	Classes	Water	Forest & dense vegetation	Shrubland & sparse vegetation	Bare land	Urban & built up area	Total
	Water	1.82	0.05	0.17	0.16	0.03	2.24
	Forest & dense veg.	0.01	594.77	357.95	50.16	0.8	1003.7
	Shrubland & sparse veg.	0.04	157.14	1077.03	200.66	6.42	1441.3
	Bare land	0.3	16.77	694.56	1192.23	18.38	1922.3
	Urban & built up area	0	0.03	2.3	4.96	6.7	13.99
	Total	2.17	768.76	2132	1448.17	32.33	4383.9

the development of effective mitigation techniques and land use planning.

Although our approach is solid, there are a few things to be aware of; first, the temporal and spatial resolution of our research was restricted by the lack of high-quality satellite images.

Secondly, various parameters, including spatial resolution, spectral characteristics, and classification algorithms, may affect the precision of LULC classification (Shi et al., 2025).

Lastly, the reliability of our findings may be impacted by uncertainties related to data preprocessing and classification errors (Cánibe et al., 2022).

Further studies needs to concentrate on tackling the detected constraints and investigating supplementary elements driving land use and land cover transformations, like socio-economic processes, land tenure structures, and policy measures. Assessments of LULC change detection can be made more accurate and reliable by incorporating participatory mapping methods, machine learning algorithms, and sophisticated remote sensing techniques (Zafar et al., 2024). Moreover, multidisciplinary research incorporating ecological, social, and economic viewpoints is required to create sustainable land management plans and lessen the negative effects of changing land cover on ecosystems and human welfare.

CONCLUSIONS

The main objective of this study was to produce and provide a standardized multi-decadal LULC change analysis for the study area (northern central Rif of Morocco) by using three temporal snapshots (2000, 2014 and 2025), with a consistent classification scheme and a strict evaluation of accuracy for each class. This goal was accomplished, producing three comparable maps with overall accuracies ranging from 87.5% to 90.8% and Kappa coefficient between 0.82 and 0.87, guaranteeing strong cross-temporal comparisons.

The analysis revealed noticeable patterns. Between year 2000 and year 2025, forest cover decreased by 5.36%, primarily on western parts of the study area where forests are abundant and slopes are high, while Built-up areas expanded

by 0.42%, particularly in the urban areas. These findings provide the first spatially explicit, multi-decadal evidence of land cover transitions in the central Rif, and help us to gain a deep understanding of the complex interactions between natural processes and human activities, and how these dynamics jointly influence and modify landscapes and ecosystems.

By addressing the gap of limited temporal coverage and inconsistent classification in prior studies, this work establishes a robust baseline for future environmental monitoring. The findings provide essential foundational data for upcoming studies and opens new prospects for integrating LULC change data into landslide susceptibility modelling, erosion risk mapping, and land management strategies, offering decision-makers a reliable tool for mitigating environmental degradation in this erosion-prone mountainous region.

Therefore, integrating concise and detailed LULC data into landslide mapping can accurately enhance our understanding of how land cover variations affect slope stability and support better risk mitigation strategies.

REFERENCES

1. Abbas Taati, F. S. (2015). Land use classification using support vector machine and maximum likelihood algorithms by Landsat 5 TM images. *8*, *12*, *Walailak Journal of Science and Technology*. https://doi.org/10.14456/WJST.2015.33
2. Abel-Schaad, D., Iriarte, E., López-Sáez, J. A., Pérez-Díaz, S., Sabariego Ruiz, S., Cheddadi, R., Alba-Sánchez, F. (2018). Are *Cedrus atlantica* forests in the Rif Mountains of Morocco heading towards local extinction? *The Holocene*, *28*(6), 1023–1037. https://doi.org/10.1177/0959683617752842
3. Ben-Said, M., Chemchaoui, A., Etebaai, I., Taher, M. (2025). Land use and land cover changes in Morocco: Trends, research gaps, and perspectives. *GeoJournal*, *90*(1), 44. https://doi.org/10.1007/s10708-024-11214-3
4. Bhargava, A. (2019). Climate change, demographic pressures and global sustainability. *Economics & Human Biology*, *33*, 149–154. https://doi.org/10.1016/j.ehb.2019.02.007
5. Bruce, C. M., Hilbert, D. W. (2004). *Pre-processing methodology for application to Landsat TM/ETM+ imagery of the Wet Tropics* 44. Cooperative Research Centre for Tropical Rainforest Ecology and Management. https://rainforest-crc.jcu.edu.au/publications/landsat_preprocessing.pdf
6. Cánibe, M., Titeux, N., Domínguez, J., Regos, A. (2022). Assessing the uncertainty arising from standard land-cover mapping procedures when modelling species distributions. *Diversity and Distributions*, *28*(4), 636–648. https://doi.org/10.1111/ddi.13456
7. Chavez Jr, P. S. (1989). Radiometric calibration of Landsat Thematic Mapper multispectral images. *Article*, 1285–1294.
8. Chavez, P. S. (1988). An improved dark-object subtraction technique for atmospheric scattering correction of multispectral data. *Remote Sensing of Environment*, *24*(3), 459–479. https://doi.org/10.1016/0034-4257(88)90019-3
9. Chavez, P. S. (1996). Image-based atmospheric corrections – Revisited and improved. *Photogrammetric Engineering and Remote Sensing*, *62*(9), 1025–1036.
10. Chen, L., Guo, Z., Yin, K., Shrestha, D. P., Jin, S. (2019). The influence of land use and land cover change on landslide susceptibility: A case study in Zhushan Town, Xuan'en County (Hubei, China). *Natural Hazards and Earth System Sciences*, *19*(10), 2207–2228. https://doi.org/10.5194/nhess-19-2207–2019
11. Cheng, G., Huang, Y., Li, X., Lyu, S., Xu, Z., Zhao, Q., Xiang, S. (2023). *Change Detection Methods for Remote Sensing in the Last Decade: A Comprehensive Review* (Version 1). arXiv. https://doi.org/10.48550/ARXIV.2305.05813
12. Congalton, R. G. (1991). A review of assessing the accuracy of classifications of remotely sensed data. *Remote Sensing of Environment*, *37*(1), 35–46. https://doi.org/10.1016/0034-4257(91)90048-B
13. Congalton, R. G., Green, K. (2008). *Assessing the Accuracy of Remotely Sensed Data: Principles and Practices, Second Edition* (0 edn). CRC Press. https://doi.org/10.1201/9781420055139
14. Congedo, L. (2016). *Semi-Automatic Classification Plugin Documentation* [Software documentation / User manual]. University of Rome 'La Sapienza'.
15. Das, S., Angadi, D. P. (2022). Land use land cover change detection and monitoring of urban growth using remote sensing and GIS techniques: A micro-level study. *GeoJournal*, *87*(3), 2101–2123. https://doi.org/10.1007/s10708-020-10359-1
16. Das, S., Sarkar, R. (2019). Predicting the land use and land cover change using Markov model: A catchment level analysis of the Bhagirathi-Hugli River. *Spatial Information Research*, *27*(4), 439–452. https://doi.org/10.1007/s41324-019-00251-7
17. Dong, S., Chen, Z., Gao, B., Guo, H., Sun, D., Pan, Y. (2020). Stratified even sampling method for accuracy assessment of land use/land cover classification: A case study of Beijing, China. *International Journal of Remote Sensing*, *41*(16), 6427–6443. https://doi.org/10.1080/01431161.2020.1739349

18. Driouech, F., Stafi, H., Khouakhi, A., Moutia, S., Badi, W., ElRhaz, K., Chehbouni, A. (2021). Recent observed country-wide climate trends in Morocco. *International Journal of Climatology*, *41*(S1). https://doi.org/10.1002/joc.6734
19. El Idrissi, M. C., Saber, E.-R., Al Mashoudi, A. (2024). Land use and land cover change analysis using geospatial techniques a case study of the Dayet Aoua Watershed, Middle Atlas, Morocco. *Environmental & Socio-Economic Studies*, *12*(4), 45–56. https://doi.org/10.2478/environ-2024-0024
20. Erbek, F. S., Özkan, C., Taberner, M. (2004). Comparison of maximum likelihood classification method with supervised artificial neural network algorithms for land use activities. *International Journal of Remote Sensing*, *25*(9), 1733–1748. https://doi.org/10.1080/0143116031000150077
21. Esri. (2020). *ArcMap* (Version 10.8) [Computer software]. Environmental Systems Research Institute. https://www.esri.com/en-us/arcgis/products/arcgis-desktop/overview
22. FAO. (2022). *The State of the World's Land and Water Resources for Food and Agriculture 2021 – Systems at breaking point*. FAO. https://doi.org/10.4060/cb9910en
23. Gashu, K., Gebre-Egziabher, T. (2018). Spatiotemporal trends of urban land use/land cover and green infrastructure change in two Ethiopian cities: Bahir Dar and Hawassa. *Environmental Systems Research*, *7*(1), 8. https://doi.org/10.1186/s40068-018-0111-3
24. He, X., Liang, J., Zeng, G., Yuan, Y., Li, X. (2019). The Effects of Interaction between Climate Change and Land-Use/Cover Change on Biodiversity-Related Ecosystem Services. *Global Challenges*, *3*(9), 1800095. https://doi.org/10.1002/gch2.201800095
25. Jensen, J. R. (2016). *Introductory digital image processing: A remote sensing perspective* (4th ed). Pearson Education.
26. Maxwell, A. E., Warner, T. A., Guillén, L. A. (2021). Accuracy assessment in convolutional neural network-based deep learning remote sensing studies—part 1: literature review. *Remote Sensing*, *13*(13), 2450. https://doi.org/10.3390/rs13132450
27. Michard, A., Saddiqi, O., Chalouan, A., Lamotte, D. F. D. (Eds). (2008). *Continental Evolution: The Geology of Morocco: Structure, Stratigraphy, and Tectonics of the Africa-Atlantic-Mediterranean Triple Junction* 116. Springer Berlin Heidelberg. https://doi.org/10.1007/978-3-540-77076-3
28. Millennium Ecosystem Assessment (Ed.). (2005). *Ecosystems and human well-being: Synthesis*. Island Press.
29. Mouddou, A., Taher, M., Etebaai, I. (2024). Diachronic Study of Coastal Vegetation Cover in Al Hoceima (Morocco): A Geospatial Analysis Using Remote Sensing and GIS. *E3S Web of Conferences*, *502*, 03008. https://doi.org/10.1051/e3sconf/202450203008
30. Muselli, M., Lekouch, I., Beysens, D. (2022). Physical and chemical characteristics of dew and rain in North-West Africa with focus on Morocco: Mapping past and future evolution (2005–2100). *Atmosphere*, *13*(12), 1974. https://doi.org/10.3390/atmos13121974
31. Naikoo, M. W., Rihan, M., Ishtiaque, M., Shahfahad. (2020). Analyses of land use land cover (LULC) change and built-up expansion in the suburb of a metropolitan city: Spatio-temporal analysis of Delhi NCR using landsat datasets. *Journal of Urban Management*, *9*(3), 347–359. https://doi.org/10.1016/j.jum.2020.05.004
32. Norovsuren, B., Tseveen, B., Batomunkuev, V., Renchin, T., Natsagdorj, E., Yangiv, A., Mart, Z. (2019). Land cover classification using maximum likelihood method (2000 and 2019) at Khandgait valley in Mongolia. *IOP Conference Series: Earth and Environmental Science*, *381*(1), 012054. https://doi.org/10.1088/1755-1315/381/1/012054
33. Nunez, S., Alkemade, R. (2021). Exploring interaction effects from mechanisms between climate and land-use changes and the projected consequences on biodiversity. *Biodiversity and Conservation*, *30*(12), 3685–3696. https://doi.org/10.1007/s10531-021-02271-y
34. Oliver, T. H., Morecroft, M. D. (2014). Interactions between climate change and land use change on biodiversity: Attribution problems, risks, and opportunities. *WIREs Climate Change*, *5*(3), 317–335. https://doi.org/10.1002/wcc.271
35. Pacheco, A. D. P., Da Silva Junior, J. A., Ruiz-Armenteros, A. M., Henriques, R. F. F., De Oliveira Santos, I. (2023). Analysis of spectral separability for detecting burned areas using Landsat-8 OLI/TIRS images under different biomes in Brazil and Portugal. *Forests*, *14*(4), 663. https://doi.org/10.3390/f14040663
36. Patra, S., Sahoo, S., Mishra, P., Mahapatra, S. C. (2018). Impacts of urbanization on land use /cover changes and its probable implications on local climate and groundwater level. *Journal of Urban Management*, *7*(2), 70–84. https://doi.org/10.1016/j.jum.2018.04.006
37. Pimentel, D. (1991). Global warming, population growth, and natural resources for food production. *Society & Natural Resources*, *4*(4), 347–363. https://doi.org/10.1080/08941929109380766
38. Prestele, R., Arneth, A., Bondeau, A., de Noblet-Ducoudré, N., Pugh, T. A. M., Sitch, S., Stehfest, E., Verburg, P. H. (2017). Current challenges of implementing anthropogenic land-use and land-cover change in models contributing to climate change assessments. *Earth System Dynamics*, *8*(2), 369–386. https://doi.org/10.5194/esd-8-369-2017

39. QGIS Development Team. (2024). *QGIS Geographic Information System* (Version 3.34) [Computer software]. Open Source Geospatial Foundation Project. https://qgis.org
40. R. Anderson, J., E. Hardy, E., T. Roach, J., E. Witmer, R. (1976). *A Land Use and Land Cover Classification System for Use with Remote Sensor Data* (Professional Paper) [Geological Survey Professional Paper 964].
41. Rasmussen, K. (1993). Methodologies and software for satellite image processing: User needs and development trends. *United Nations Publication Series A*, 1–14.
42. Roy, D. P., Wulder, M. A., Loveland, T. R., C.E., W., Allen, R. G., Anderson, M. C., Helder, D., Irons, J. R., Johnson, D. M., Kennedy, R., Scambos, T. A., Schaaf, C. B., Schott, J. R., Sheng, Y., Vermote, E. F., Belward, A. S., Bindschadler, R., Cohen, W. B., Gao, F., … Zhu, Z. (2014). Landsat-8: Science and product vision for terrestrial global change research. *Remote Sensing of Environment*, *145*, 154–172. https://doi.org/10.1016/j.rse.2014.02.001
43. Salhi, A., Martin-Vide, J., Benhamrouche, A., Benabdelouahab, S., Himi, M., Benabdelouahab, T., Casas Ponsati, A. (2019). Rainfall distribution and trends of the daily precipitation concentration index in northern Morocco: A need for an adaptive environmental policy. *SN Applied Sciences*, *1*(3), 277. https://doi.org/10.1007/s42452-019-0290-1
44. Sang, C. C., Olago, D. O., Ongeri, Z. J. (2023). The factors driving land cover transitions and land degradation and the potential impacts of the proposed developments in the Isiolo dam watershed, LAPSSET corridor, Kenya. *Discover Sustainability*, *4*(1), 9. https://doi.org/10.1007/s43621-023-00126-w
45. Shi, Y., Jin, N., Wu, B., Wang, Z., Wang, S., Yu, Q. (2025). Effects of machine learning models and spatial resolution on land cover classification accuracy in Dali County, Shaanxi, China. *International Journal of Agricultural and Biological Engineering*, *18*(1), Article 1. https://doi.org/10.25165/ijabe.v15i5.7252
46. Storey, J., Choate, M., Lee, K. (2014). Landsat 8 Operational Land Imager On-Orbit Geometric Calibration and Performance. *Remote Sensing*, *6*(11), 11127–11152. https://doi.org/10.3390/rs61111127
47. Suter, G. (1980). *Carte structurale de la chaîne rifaine au 1/500 000* (Notes et Mémoires du Service géologique du Maroc No. 245b). Service géologique du Maroc.
48. Talukdar, S., Singha, P., Mahato, S., Shahfahad, Pal, S., Liou, Y.-A., Rahman, A. (2020). Land-use land-cover classification by machine learning classifiers for satellite observations—a review. *Remote Sensing*, *12*(7), 1135. https://doi.org/10.3390/rs12071135
49. Tan, L., L. K., R. T., Zhang, Z. (2024). Analysis of land use/land cover changes and driving forces during the period 1992–2022: A case study of Jinan City, China. *AQUA — Water Infrastructure, Ecosystems and Society*, *73*(3), 584–607. https://doi.org/10.2166/aqua.2024.311
50. Tariq, M. (2024). Effects of population pressure and excessive cultivation on climate change in District Dir (Lower) Khyber Pakhtunkhwa: Perception of local farming community. *Kurdish Studies*, 1130–1142. https://doi.org/10.53555/ks.v12i4.3125
51. Teillet, P. M., Guindon, B., Goodenough, D. G. (1982). On the slope-aspect correction of multispectral scanner data. *Canadian Journal of Remote Sensing*, *8*(2), 84–106. https://doi.org/10.1080/07038992.1982.10855028
52. Vali, A., Comai, S., Matteucci, M. (2020). Deep learning for land use and land cover classification based on hyperspectral and multispectral earth observation data: a review. *Remote Sensing*, *12*(15), 2495. https://doi.org/10.3390/rs12152495
53. Venter, Z. S., Sydenham, M. A. K. (2021). *Continental-scale land cover mapping at 10 m resolution over Europe (ELC10)*. https://doi.org/10.48550/ARXIV.2104.10922
54. Xie, H., Huang, H. (2022). Classification of land cover remote-sensing images based on pattern recognition. *Scientific Programming*, *2022*, 1–15. https://doi.org/10.1155/2022/8319692
55. Zafar, Z., Zubair, M., Zha, Y., Fahd, S., Nadeem, A. A. (2024). Performance assessment of machine learning algorithms for mapping of land use/land cover using remote sensing data. *The Egyptian Journal of Remote Sensing and Space Sciences*, *27*(2), 216–226. https://doi.org/10.1016/j.ejrs.2024.03.003